ELSEVIER

Biochimica et Biophysica Acta 1320 (1997) 73–82

BIOCHIMICA ET BIOPHYSICA ACTA
BBA

A small-angle neutron scattering study on the small aggregates of bacteriochlorophylls in solutions

Zheng-Yu Wang [a,*], Mitsuo Umetsu [a], Kenji Yoza [a], Masayuki Kobayashi [a], Masayuki Imai [b], Yushu Matsushita [b], Nobuo Niimura [c], Tsunenori Nozawa [a]

[a] *Department of Biochemistry and Engineering, Faculty of Engineering, Center for Interdisciplinary Science, Tohoku University, Aoba-ku, Sendai 980-77, Japan*
[b] *Institute for Solid State Physics, University of Tokyo, Tokai, Naka, Ibaraki, 319-11, Japan*
[c] *Advanced Science Research Center, JAERI, Ibaraki 319-11, Japan*

Received 31 October 1996; revised 24 January 1997; accepted 27 January 1997

Abstract

Small-angle neutron scattering measurements have been made to determine the size of small aggregates of bacteriochlorophyll (BChl) *a* and *c* formed in non-polar solution. Both BChl *a* and *c* form dimers and oligomers in equilibrium with each other at high concentrations in benzene-d_6 solutions. The size and molecular weight for each dimer have been quantitatively evaluated based on Guinier approximation. The radii of gyration of the dimers are determined to be 17.0 ± 0.5 Å and 16.5 ± 0.5 Å for the BChl *a* and *c*, respectively. Limited observations in the very small angle region suggest that the oligomers are of considerable dimension, approximately as large as a hundred angstroms for the radius of gyration. The SANS results can be well correlated with the electronic absorption and NMR spectra and are in good agreement with other spectroscopic behavior of the small aggregates reported previously.

Keywords: Pigment aggregation; Small-angle neutron scattering; Green bacterium; Antenna; Chlorosome; Radius of gyration

1. Introduction

Aggregation phenomena of bacteriochlorophylls (BChl) and chlorophylls (Chl) are of particular interest in relation to the organization of these molecules in photosynthetic systems. Common features observed in various BChl and Chl aggregates in vitro result from the nature of preference of the central magnesium ion for five- or sixfold coordination [1–3]. Since only four sites are occupied by the pyrrole nitrogens in the pigment macrocycle, the coordinative unsaturation must be satisfied by an additional one or two axial ligand depending on the solvent properties. In polar solvents, such as acetone and methanol, BChl and Chl are monomeric with solvent molecules coordinated axially to one or both sites of the magnesium. In non-polar solvents, such as benzene and carbon tetrachloride, the pigments occur as dimer or oligomer in which the vacant coordination sites on the magnesium atom of a pigment molecule are satisfied by a second pigment molecule directly using a carbonyl or hydroxyl group, or indirectly via a water molecule [4,5]. The aggregation behavior can

---

Abbreviations: BChl, bacteriochlorophyll; Chl, chlorophyll; SANS, small-angle neutron scattering; CD, circular dichroism.

[*] Corresponding author. Fax: (81) (22) 217-7293; E-mail: wang@biophys.che.tohoku.ac.jp

PII S0005-2728(97)00014-5

be described in terms of a strongly solvent-dependent monomer ↔ dimer ↔ oligomer equilibrium [6,7]. The formation of certain types of oligomer is accompanied by a bathochromic shift of the long-wavelength absorption band (Q_y) with respect to that of monomeric form in polar solvents.

BChl *a* is the major chlorophyll of purple bacteria. NMR titration study suggested that BChl *a* exist in dimeric form in benzene [3]. Aggregation behavior of BChl *a* in carbon tetrachloride was interpreted as a trimer ↔ hexamer equilibrium mixture by observation of vapor-phase osmometry, and BChl *a* appears to exist as a trimer in dilute solution [8]. This result is in contrast to the conclusion derived from absorption spectroscopy that Chl *a*, *b* and BChl *a* occur as dimers with much the same structure [9]. Oligomers of BChl *a* can be formed in mixed aqueous-organic solvent systems, such as water/formamide, and in aqueous micelles of the detergent lauryldimethylamine oxide [10]. It has been well established that the aggregation of BChl *a*, like most other Chl, involves strong, coordinative interaction of the central magnesium of one pigment with a 13^1-carbonyl functional group of the second as an electron donor [4–7,11–13]. In addition, the acetyl carbonyl at position 3^1 is also involved in aggregate formation in high concentration range [9]. In contrast, BChl *c* is the major pigment of green photosynthetic bacteria. It lacks the 13^2-carbomethoxy group and can be regarded as a pyrochlorophyll. The most significant differences in the molecular structures between BChl *c* and BChl *a* is probably the existence of a 3^1-hydroxyl group (Fig. 1). There is strong evidence that this group is involved in the aggregation, with the 3^1-hydroxyl oxygen coordinating to the magnesium atom of a second BChl *c* molecule [14–27]. Furthermore, unlike BChl *a*, a small amount of water does not seem to markedly affect the properties of BChl *c* aggregates. This is probably because the BChl *c* molecule has a nucleophilic group (3^1-hydroxyl) as a part of the molecule, and lacks the 13^2-carboxymethyl substituent linked by a water molecule.

Although spectroscopic studies have provided a wealth of information about the pigment-pigment and pigment-solvent interactions at the molecular level, efforts to deduce the size of small aggregates of BChl from spectral measurements are subject to some ambiguity since the state of aggregation in non-polar solvents is highly variable. The analysis of small-angle neutron scattering (SANS) data to be described in the present article provides further quantitative information about the dimension and molecular weight of the small BChl aggregates in benzene solutions in order to facilitate the interpretation of electronic absorption and NMR spectra of these pigments in solution. The reason for using benzene as a solvent is that solvents containing chlorine strongly absorb neutrons which causes a low signal-to-noise ratio, while benzene-d_6 has low background of neutron scattering and can produce various aggregates with very similar spectral properties to those in CCl_4. The results of this study confirm and amplify many of the previous

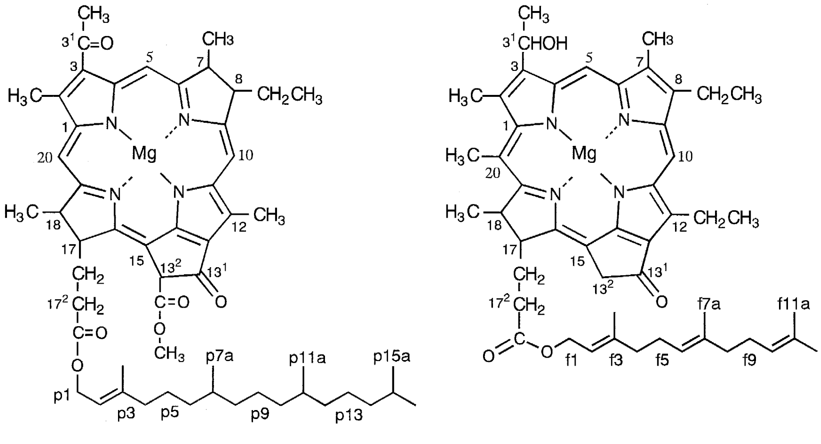

Fig. 1. Molecular structures of BChl *a* and *c*.

findings and represent independent evidence for the existence of dimers and oligomers in the concentrated solutions. Similar SANS studies have also been made on the suspension of very large aggregates of Chl and BChl in aqueous solutions by Worcester et al. [28,29]. Based on their results, a micelle-like cylinderic structure has been proposed with the size of at least 200 nm in length and about 5 ~ 10 nm in radius. Comparing to the large aggregates, we refer to the dimer and oligomers of this study as small aggregates.

2. Experimental

2.1. Materials

BChl *a* was extracted from *Chromatium tepidum*. Lyophilized cells (2 ~ 3 g) were ground to a powder and extracted with 50 ml of methanol for three times. The extract was filtered through a Buchner funnel and concentrated by evaporation to a final volume of 2 ~ 3 ml. The concentrated extract was chromatographed on a reversed phase HPLC column with a dimension of 21.5 mm in diameter and 30 cm in length (TOSOH, TSKgel ODS-80Ts). Eluted BChl *a*/methanol solution was evaporated, and the residual methanol was further removed by blowing N_2 steam for more than 30 min. The purified BChl *a* was checked by ^{1}H-NMR and absorption spectra. All procedures were carried out in dim light or darkness and were completed as rapidly as possible to minimize degradation. Spectral grade methanol was used for the extraction without further purification. BChl *c* was extracted from dry cells of *Chlorobium tepidum* with methanol and purified as described previously[25]. The extracted BChl *c* was characterized by NMR and absorption spectra. Deuterated benzene (purity > 99.7%, $D > 99.5\%$, Merck) and deuterated acetone ($D > 99.9\%$, Isotec) were used for SANS and NMR experiments. Other solvents were spectral grade. BChl *a* and *c* solutions were prepared by dissolving the dried pigments in benzene-d_6 or acetone-d_6 (≈ 3 mg/ml), then passing through a membrane filter (TOYO, PTFE, 0.22 μm).

2.2. SANS measurements

SANS experiments were performed on the instrument (SANS-U) installed in JRR-3M of Japan Atomic Energy Research Institute (JAERI). The neutron beam from a cold source was monochromatized by a velocity selector (Dornier). Scattered neutrons were led to a evacuated scattering flight tube and recorded using a two-dimensional position-sensitive detector (Ordela) with an active area of 65×65 cm^2 and resolution of 5×5 mm^2. The 2D data were radially averaged and converted as a function of $Q = 4\pi \sin\theta/\lambda$, where θ is half the scattering angle and λ is the wavelength ($\lambda = 7.0$ Å). The sample-to-detector distance was 2 m. Details on specification of the instrument were described elsewhere [30]. The raw data were corrected for solvent background, transmission and incoherent scattering, and finally were normalized to absolute intensity units (cm^{-1}) using Lupolen as a reference [31]. The sample solutions were placed in a quartz cell of 4 mm path length at 23°C.

The SANS data were analyzed by using standard Guinier analysis [32], i.e., the scattered intensity is expected to vary as

$$I(Q) = I(0)\exp\left(-R_g^2 Q^2/3\right) \tag{1}$$

in the region of $QR_g \leq 1$. Slope of the plot ($\ln I(Q)$ vs. Q^2) yields the radius of gyration R_g of the aggregate, and the y-intercept yields $I(0)$, the scattering intensity at 0° angle. R_g is defined by

$$R_g^2 = \frac{\int r^2[\rho(r) - \rho_s]\mathrm{d}^3r}{\int[\rho(r) - \rho_s]\mathrm{d}^3r} \tag{2}$$

where $\rho(r)$ is the local scattering-length density of the solvent-excluded particle and ρ_s is the solvent scattering-length density. $I(0)$ contains information on M/m^2, where M is the molar mass of the entire aggregate, and m that of a single monomer unit [33].

$$I(0) = N_a c[b_1 - (v_1/v_2)b_2]^2 M/m^2 \tag{3}$$

In Eq. (3), N_a is Avogadro's number, c is the concentration of aggregate, 1 and 2 ($= i$) represent the aggregate and solvent respectively, b_i is the sum of the nuclear coherent scattering lengths of component i, and v_i is the partial molar volume of i. Since no D-H exchange between the aggregate and the solvent is expected, the scattering lengths can be calculated and the values of the constant parameters are given in Table 1. The partial molar volume for the pigments was calculated using the specific density of the crystalline Chl *a* [34].

Table 1
Relevant parameters for systems considered for SANS

Component	Specific density (g/cm^3)	Scattering length ($\times 10^{-12}$, cm)	Scattering length density ($\times 10^{10}$, cm^{-2})
BChl *a*	1.08 [a]	16.6	1.19
BChl *c*	1.08 [a]	16.6	1.34
BChlorin *a*	1.28 [b]	17.9	2.22
BChlorin *c*	1.28 [b]	16.0	2.08
Phytyl	0.850 [c]	−1.30	−0.239
Farnesyl	0.887 [d]	0.617	0.161
Acetone-d$_6$	0.872	6.58	5.39
Benzene-d$_6$	0.95	7.99	5.43

[a] The value for microcrystalline Chl *a* [34].
[b] The value for crystal of ethyl chlorophyllide *a* [35].
[c] Estimated from the density of phytol.
[d] Estimated from the density of farnesol.

2.3. Spectroscopic measurements

UV-vis absorption spectra were recorded using the same spectrometer under similar conditions as those described in a previous paper [36]. Deconvolution of the spectra was made by a home-made program based on the least-squares method [37]. ^{1}H-NMR spectra were measured on a Bruker DPX-400 spectrometer, using a 30° pulse, a pulse repetition time of 2 s, and 800 scans. The solution sample was placed in a 5 mm NMR tube, and the chemical shifts were referred to TMS.

3. Results

3.1. Estimation of the sizes of small aggregates by SANS

Fig. 2 shows the Guinier plots of the measured neutron scattering spectra for BChl *a* in benzene-d$_6$ and acetone-d$_6$. A good linearity was found for the BChl *a* in acetone-d$_6$ over the whole range of Q ($Q = 0.01 \sim 0.15$ Å^{-1}), as expected for a monodisperse solution without interparticle interaction. This is in agreement with the fact that BChl *a* exists as a monomer in acetone solution. The size of the monomers is characterized by the radius of gyration, R_g, obtained from the Guinier plot. A value of $R_g = 10.0 \pm 0.5$ Å was determined from the slope for the BChl *a* monomer in acetone-d$_6$. The relationship between R_g and actual molecular dimension depends upon the shape of particles. For the BChl *a* in benzene-d$_6$, the measured neutron scattering spectrum can be clearly divided into two parts. The first part is in the region $Q > 0.03$ Å^{-1}, where the Guinier

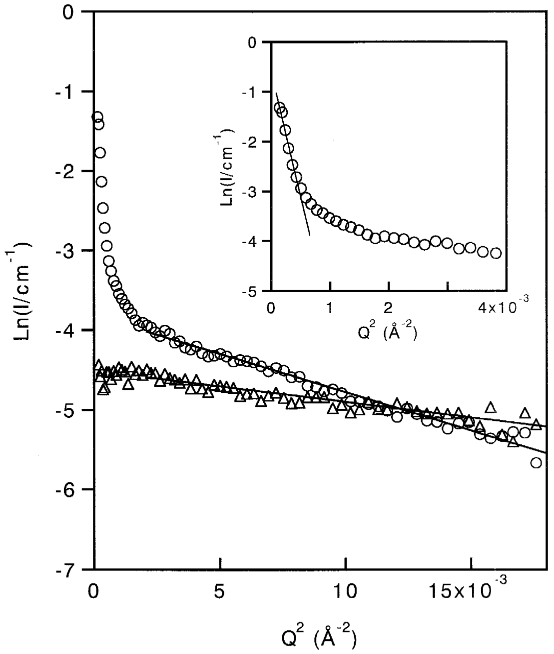

Fig. 2. Guinier plots of the corrected SANS spectra from BChl *a* in benzene-d$_6$ (○) and in acetone-d$_6$ (△) solutions. BChl *a* concentration for each solution was 3.2 mM. The straight lines are the fitted data according to Guinier approximation to determine the radius of gyration and the scattering amplitude. Inset is the enlargement of very small Q region for BChl *a* in benzene-d$_6$.

plot shows a good linearity with a slope steeper than that for BChl *a* in acetone. This is an indication of the existence of small aggregates. The value of R_g was determined to be 17.0 ± 0.5 Å. This is believed to correspond to a partially overlapped dimer. Calculation from the intercept of the linear plot also showed that molecular weight of the small aggregates is about twice (2.08) that for BChl *a* monomer in acetone. The other part of the neutron scattering spectrum is in the very small Q region, about $Q < 0.03$ Å^{-1}, where the neutron scattering intensity increased rapidly with decreasing Q. This indicates the existence of oligomers with R_g values at least several tens Ångstroms. Applying the Guinier plot to the relatively linear part, as shown in the inset of Fig. 2, gave a value of about 107 Å for R_g. However, the exact values of R_g and $I(0)$ for these oligomers cannot be determined accurately from the measured neutron scattering intensities because of insufficient data in the very small Q region. The strong neutron scattering in this region is not due to strong interparticle interactions since the BChl *a* concentration was the same as that of acetone solution (3.2 mM).

Similar results were observed for BChl *c* and are shown in Fig. 3. The Guinier's law held over the whole range of Q for the BChl *c* in acetone-d_6. The fitted straight line gave a R_g value of 10.5 ± 0.5 Å. It is known that BChl *c* exists as a monomer in acetone, and the R_g value is compatible with that of BChl *a*. For BChl *c* in benzene-d_6, the Guinier plot was dominated by a wide linear region at $Q > 0.02$ Å^{-1}, where a value of 16.5 ± 0.5 Å was obtained for the radius of gyration. The small aggregates were estimated to be dimers by taking into account the molecular weight calculated from the intercept. The existence of larger oligomers was also confirmed from the Guinier plot in a very small Q region ($Q < 0.02$ Å^{-1}), where a very rough value of 96 Å was estimated for the radius of gyration.

For all cases, the neutron scattering intensities can be fitted with straight lines in the region of $Q^2 > 0.0009$ Å^{-2} according to Eq. (1) to determine R_g and $I(0)$ for the monomers and dimers. Oligomers with R_g values of about 100 Å can only be roughly estimated from the intensity data in the very small Q region. Large aggregates with R_g values exceeding 100 Å should contribute very little to the neutron scattering intensities in the region $Q > 0.03$ Å^{-1}, but will slightly affect the accuracy of the values of R_g and $I(0)$ for the small aggregates as determined by the Guinier approximation. The neutron scattering results showed that both BChl *a* and BChl *c* exist as monomers in acetone and form small aggregates (dimers and oligomers) in benzene with the similar sizes, even though the interaction mode involved in the aggregates is considered to be different between BChl *a* and BChl *c*. The results also suggested that both the dimers and oligomers are quite stable and exist in an equilibrium of $(\mathrm{BChl})_2 \leftrightarrow (\mathrm{BChl})_n$ at high concentrations in benzene solution.

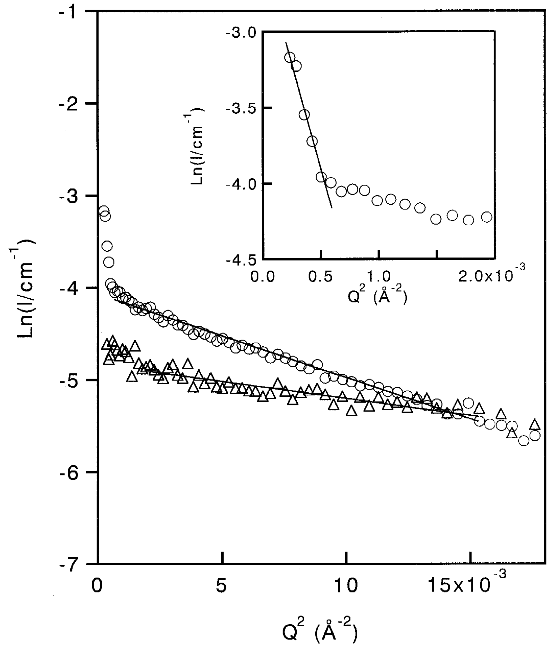

Fig. 3. Guinier plots of the corrected SANS spectra from BChl *c* in benzene-d_6 (○) and in acetone-d_6 (△) solutions. BChl *c* concentrations in benzene and in acetone were 4.9 mM and 4.1 mM, respectively. The straight lines are the fitted data according to Guinier approximation to determine the radius of gyration and the scattering amplitude. Inset is the enlargement of very small Q region for BChl *c* in benzene-d_6.

3.2. Spectral properties of the small aggregates

Fig. 4a shows optical absorption spectra of the BChl *a* samples used for SANS measurement (Fig. 2). BChl *a* in acetone showed a single Q_y band at 770 nm corresponding to the monomeric form, whereas BChl *a* in benzene had a Q_y band at 780 and a shoulder around 815 nm, implying an occurrence of two components as a result of aggregate formation. It is noteworthy that the spectrum of BChl *a* in benzene closely resembles that in CCl_4 [4,9]. The aggregate spectrum in the near infrared region was deconvoluted and the result is shown in Fig. 4b. Two peaks at 781 nm and 817 nm were assigned to the $Q_{y0\text{-}0}$ bands of the two components. Proportion of the two components is known to vary with the pigment concentration [3]. In order to prove that the 781nm-component is not a monomeric form, the spectral properties at low concentration (0.18 mM) in benzene were investigated and the results are shown in Fig. 5. Absorption spectrum in the near infrared region was dominated by the 781 nm peak with only trace 815 nm component (Fig. 5a). Most significant changes of BChl *a* from monomer to dimer or oligomer can be observed with the low-field signals of corresponding ^{1}H-NMR spectra (Fig. 5b). In benzene, the 13^2-proton markedly shifted to the higher field by 0.67 ppm and meso-proton at position 5 shifted to the lower field by 0.49 ppm with respect to those in acetone (Fig. 5c). In the meantime, line broadenings occurred for the NMR spectrum due to the rapid relaxation of protons with formation of the small aggregates. The result of this study was similar to that of NMR shift titration experiment [3] and suggested that BChl *a* exists predominantly in a dimeric form in benzene at low concentration. Therefore, the 781nm-component must be the dimer species with a R_g value of 17 Å, while the 817-nm component corresponds to the oligomer with a R_g value of about 107 Å, as identified by the SANS measurements.

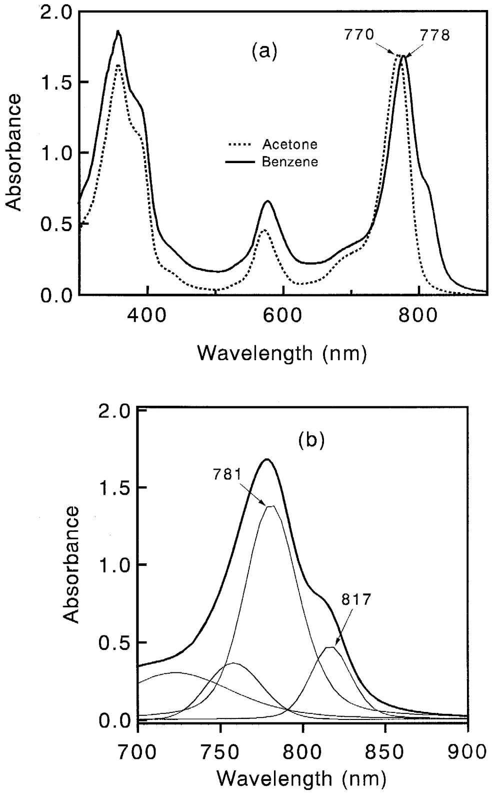

Fig. 4. a: absorption spectra of BChl *a* in benzene (solid line) and in acetone (dashed line) solutions. The samples were the same as those used in the SANS measurements. b: deconvolution of the absorption spectrum of BChl *a* in benzene in the near infrared region.

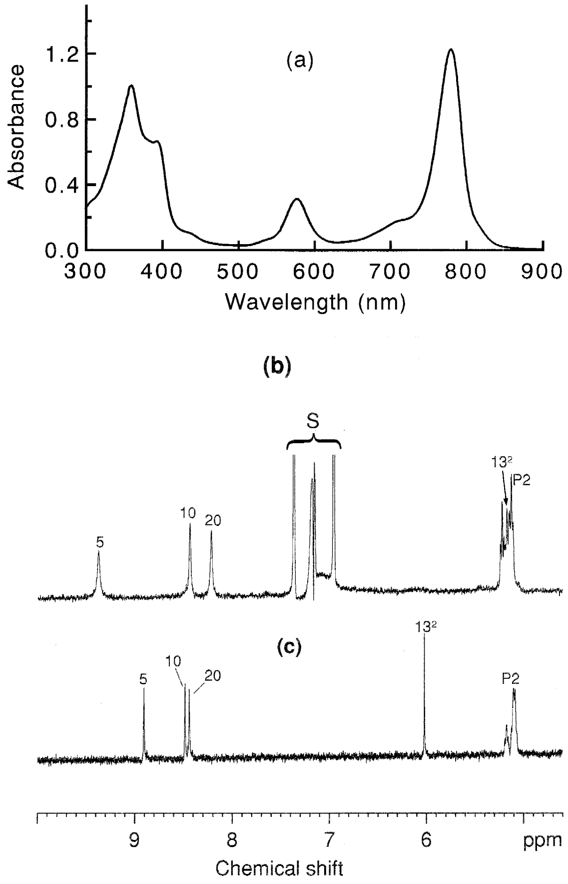

Fig. 5. a: absorption spectra of BChl *a* in benzene-d_6 at low concentration (0.18 mM). b: corresponding ^{1}H-NMR spectrum. S: undeuterated solvent signals. c: ^{1}H-NMR spectrum of BChl *a* in acetone-d_6 (0.18 mM).

Fig. 6a shows the absorption spectra of BChl *c* in acetone and benzene. The spectrum in benzene was found to drastically change with the pigment concen-

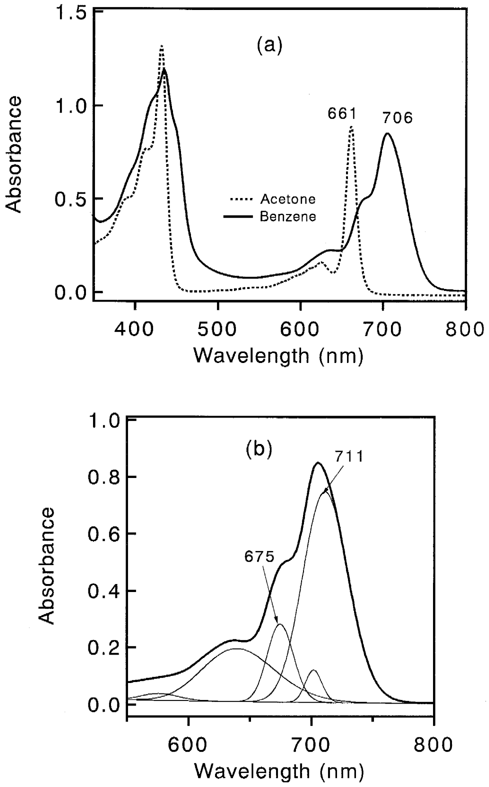

Fig. 6. a: absorption spectra of BChl *c* in benzene (solid line) and in acetone (dashed line) solutions. The samples were the same as those used in the SANS measurements. b: deconvolution of the absorption spectrum of BChl *c* in benzene in the near infrared region.

tration. At high concentrations, as the case of this study, the shape of the spectrum closely resembled that for the BChl *c* in $CHCl_3$ or CCl_4 [17,19], i.e., a shoulder at 675 nm and a peak around 710 nm. We have also carried out a ^{1}H-NMR measurement on the low concentration BChl *c*/benzene-d_6 solution and found that the spectrum was the same as that reported previously for the BChl *c* in $CDCCl_3$ [23]. Fig. 6b shows the deconvoluted spectra in the near infrared region. Two bands centered at 675 nm and 711 nm were assigned to two major components. The small aggregates were rich in the 711 nm species. The spectroscopic behavior of BChl *c* aggregates in various solutions has been well investigated by absorption spectra [17,19], NMR [20,23] and fluorescence [15,22]. There is little doubt that dimer shows an absorption peak at 675 ~ 680 nm. The component with the absorption at 710 nm, however, remains somewhat unclear. Absorption study suggested that it could be a tetramer species [19], whereas fluorescence results appeared to be better interpreted by a hexamer model [22]. Although we cannot determine the precise aggregation number of the 710 nm oligomer at this stage, the SANS results of this study have given the characteristic sizes for both dimer and oligomer, and have demonstrated that the 675nm-component should be the dimer with a R_g value of 16.5 Å and the 711-nm component is a oligomer with an approximate value of 96 Å for the radius of gyration.

4. Discussion

Direct evidence has been provided by the SANS measurements for the presence of an equilibrium between dimer and oligomer in the concentrated solutions of BChl *a* and *c* in benzene. Estimation of the size and molecular weight was based on the Guinier approximation that was found to hold over a wide *Q* range for the monomeric and dimeric species. Advantages of the Guinier approximation are that it needs no adjustable or physical parameters for the determination of radius of gyration and only a few physical parameters, such as concentration, specific densities of solute and solvent, are required for the calculation of molecular weight of the particles in solution. The values obtained for the small aggregates can be compared with those of monomers. Theoretically, the radius of gyration for a monomer can be calculated according to Eq. (2) if we know the coordinates of all atoms in the pigment molecule. Unfortunately, it is not possible to do a complete calculation on the whole BChl molecule since the conformation of its esterifying chain in solution is unknown. The size of chlorin ring, however, can be evaluated if we assume that the chlorin ring is rigid and has the same conformation as in its crystal state. Using the crystal data of ethyl chlorophyllide [35,38], a value of 5.0 Å was obtained for the radius of gyration. Hence, the R_g value of about 10 Å determined by SANS measurement is believed to be reasonable for a whole BChl molecule. The radii of gyration for the BChl dimers in benzene (16.5 Å ~ 17.0 Å) were much smaller than twice the values of monomers, suggesting that two pigment molecules are partially overlapped. This is consistent with spectroscopic results from solutions [5,9,11,13,16,39] and diffraction results from crystalline BChl and Chl aggregates [35,38].

The electronic absorption spectra of BChl *a* in benzene and in CCl_4 are very similar. Early studies on the aggregation of BChl *a* in CCl_4 by visible absorption spectroscopy suggested the existence of monomer-dimer equilibrium in the concentration range lower than 10^{-3} M [9]. A dimerization constant of 2.2×10^{-4} M^{-1} was obtained, corresponding to standard free energy of dimer formation of -24.3 kJ/mol. On the other hand, molecular weight measurements by vapor pressure osmometry demonstrated that the aggregation behavior of BChl *a* in CCl_4 appeared intermediate between that of Chl *a* and *b*, and may be better interpreted as a trimer ↔ hexamer equilibrium mixture in concentrated solutions [5]. It is well known that Chl *a* exists predominantly as dimers in benzene or CCl_4 over a wide concentration range, accompanied by varying amounts of oligomers, whereas Chl *b* is typical of trimers at concentrations lower than 10 mM [5,40,41]. It was also pointed out that conclusions derived from CCl_4 solution may not apply to the situation for the case of aromatic solvents like benzene [9]. More recently, detailed analyses of the absorption spectra and NMR titration by Brereton and Sanders clearly demonstrated that BChl *a* is dimeric in benzene [3]. Our SANS results, along with the ^{1}H-NMR result, are in satisfactory agreement with those of Brereton and Sanders. The largest change in chemical shift upon formation of BChl *a* small aggregates in benzene is for the 13^2-proton. This can be interpreted as indicating the participation of the 13^1-carbonyl of ring V in the dimer formation. The interaction is presumed to be primarily with the central magnesium of a second BChl *a* molecule. Another information on the coordinating property can be obtained from absorption spectra. Evans and Katz suggest that the position of the Q_x band is strongly dependent on the coordination state [2]. Five-coordinated Mg species absorb near 580 nm, whereas 6-coordinated Mg species are red-shifted to about 610 nm. In this study, the Q_x band was found at 572 nm in acetone and 578 nm in benzene, respectively. This confirms the observation that 5-coordination is the principal coordination state of Mg in the aggregated BChl *a* [2]. On the basis of electronic absorption, CD and NMR spectra, a molecular model for the dimer structure has been proposed [9,39,41], in which there are regions of mutual overlap in the vicinity of ring V. This is also consistent with the results of radius of gyration determined by the SANS measurement. The model further implied that the arrangement of the monomers in the dimer can hardly be in parallel planes for steric reasons, and assumed that the ring-planes intersect at a small angle.

No study has been found on the aggregation behavior of BChl *c* in benzene. However, like BChl *a*, the absorption spectrum of BChl *c* in benzene at the concentration of this study was very similar to that in CCl_4. Spectroscopic studies suggest that dimer has an absorption maximum at about 680 nm, and the dimer and higher aggregate which absorbs at about 710 nm are in equilibrium with each other in CCl_4 solution. Our results show that BChl *c* forms dimer absorbing at 675 nm and oligomer absorbing at 711 nm. The size of 675 nm-dimer has been precisely determined by SANS measurement, corresponding to the radius of gyration of 16.5 Å, while limited observations of the neutron scattering in very small angle region imply that the 711 nm-oligomer may have a dimension as large as about a hundred angstrom. Olson and Cox have concluded that the aggregation state of the 710 nm-species in CCl_4 is a tetramer formed by association of two dimers, based on deconvolution of absorption spectra of BChl *c* solutions over a range of concentrations [19]. This conclusion has later been challenged by the results from polarized fluorescence measurement. Since the measured profile of time-dependent anisotropy yields the rotational diffusion constants, molecular size and shape of the aggregates can be estimated by the Stokes–Einstein theory. Causgrove et al. showed that the observed rotational time for the 710 nm aggregate was much longer than that of the monomer, indicating that the aggregate is of considerable size [22]. Their results appeared to be best explained by a cyclic hexamer model rather than a tetramer. The closed hexamer structure consists of three identical dimers, each as a building block, and forms a triangular arrangement with a shape of oblate spheroid and an approximate dimension of 15Å × 29Å × 29Å. However, because the experiments and calculations were conducted by using a model compound, Mg-methyl bacteriopheophorbide *d*, for simplicity, the size obtained cannot be directly compared with the radius of gyration for the unmodified BChl *c* oligomer of this study, but only be used as a rough estimate for the dimension of the 710 nm aggregate formed by chlorin rings without the long farnesyl tails. The farnesyl chain is believed to play an important role in stabilizing the conformation of the interacting pigment molecules and in maintaining the structural integrity of the whole aggregate in solution. Actually, such evidence has already been observed in the fluorescence experiment that the long farnesyl tails caused a biexponential rotational relaxation which greatly complicated the analysis of rotational diffusion data [22]. In order to determine the size and molecular weight of the 710 nm oligomer, more precise SANS measurements in smaller angle region are needed. Such experiments are planned to extend this study to a wider concentration and *Q* range.

5. Conclusion

Small-angle neutron scattering has been proven to be a useful method for the measurement of molecular aggregation in BChl solutions. Both BChl *a* and *c* form dimers and oligomers in equilibrium with each other at high concentration in benzene solutions. The size and molecular weight for each dimer can be quantitatively determined based on Guinier approximation. It is shown that the radii of gyration of the dimers are nearly identical for the two BChl molecules even though the interacting mode involved in the dimers is considered to be different between BChl *a* and BChl *c*. Limited observations in the very small angle region suggest that the oligomers are of considerable dimension, approximately as large as a hundred angstroms for the radius of gyration. The SANS results can be well correlated with the spectroscopic behavior of the small aggregates and are in good agreement with those reported previously by other researchers.

Acknowledgements

This work was performed under the Inter-University Program for the Joint use of JAERI Facilities (Proposal No. 5718), and was supported by Grant-in-Aid from the Ministry of Education, Science and Culture, Japan (Nos. 07750872, 08455377).

References

[1] Miller, J.R. and Dorough, G.D. (1952) J. Am. Chem. Soc. 74, 3977–3981.

[2] Evans, T.A. and Katz, J.J. (1975) Biochim. Biophys. Acta 396, 414–426.

[3] Brereton, R.G. and Sanders, J.K.M. (1983) J. Chem. Soc. Perkin Trans. I 423–430.

[4] Dratz, E.A., Shultz, A.J. and Sauer, K. (1967) Brookheven Symp. Biol. 19, 303–318.

[5] Ballschmiter, K. and Katz, J.J. (1969) J. Am. Chem. Soc. 91, 2661–2677.

[6] Katz, J.J., Strain, H.H., Leussing, D.L. and Dougherty, R.C. (1968) J. Am. Chem. Soc. 90, 784–791.

[7] Ballschmiter, K., Cotton, T.M., Strain, H.H. and Katz, J.J. (1969) Biochim. Biophys. Acta 180, 347–359.

[8] Ballschmiter, K., Truesdell, K. and Katz, J.J. (1969) Biochim. Biophys. Acta 184, 604–613.

[9] Sauer, K., Smith, J.R.L. and Schultz, A.J. (1966) J. Am. Chem. Soc. 88, 2681–2688.

[10] Scherz, A. and Parson, W.W. (1984) Biochim. Biophys. Acta 766, 653–665.

[11] Boxer, S.G. and Closs, G.L. (1976) J. Am. Chem. Soc. 98, 5406–5408.

[12] Wasielewski, M., Smith, U.H., Cope, B.T. and Katz, J.J. (1977) J. Am. Chem. Soc. 99, 4172–4173.

[13] Bucks, R.R. and Boxer, S.G. (1982) J. Am. Chem. Soc. 104, 340–343.

[14] Bystrova, M.I., Mal'gosheva, I.N. and Krasnovskii, A.A. (1979) Mol. Biol., 13, 440–451.

[15] Brune, D.C., Nozawa, T. and Blankenship, R.E. (1986) Biochemistry 26, 8644–8652.

[16] Smith, K.M., Bobe, F.W., Goff, D.A. and Abraham, R.J. (1986) J. Am. Chem. Soc. 108, 1111–1120.

[17] Olson, J.M. and Pedersen, J.P. (1990) Photosynth. Res., 25, 25–37.

[18] Nozawa, T., Noguchi, T. and Tasumi, M. (1990) J. Biochem. 108, 737–740.

[19] Olson, J.M. and Cox, R.P. (1991) Photosynth. Res. 30, 35–43.

[20] Nozawa, T., Ohtomo, K., Takeshita, N., Morishita, Y., Osawa, M. and Madigan, M.T. (1992) Bull. Chem. Soc. Jpn. 65, 3493–3494.

[21] Causgrove, T.P., Brune, D.C. and Blankenship, R.E. (1992) J. Photochem. Photobiol. B: Biol. 15, 171–179.

[22] Causgrove, T.P., Cheng, P., Brune, D.C. and Blankenship, R.E. (1993) J. Phys. Chem. 97, 5519–5524.

[23] Nozawa, T., Ohtomo, K., Suzuki, M., Morishita, Y. and Madigan, M.T. (1993) Bull. Chem. Soc. Jpn. 66, 231–237.

[24] Hildebrandt, P., Tamiaki, H., Holzwarth, A.R. and Schaffner, K. (1994) J. Phys. Chem. 98, 2192–2197.

[25] Nozawa, T., Ohtomo, K., Suzuki, M., Nakagawa, H., Shikama, Y., Konami, H. and Wang, Z.-Y. (1994) Photosynth. Res. 41, 211–223.
[26] Holzwarth, A.R. and Schaffner, K. (1994) Photosynth. Res. 41, 225–233.
[27] Chiefari, J., Griebenow, K., Griebenow, N., Balaban, T.S., Holzwarth, A.R. and Schaffner, K. (1995) J. Phys. Chem. 99, 1357–1365.
[28] Worcester, D.L. Michalski, T.J. and Katz, J.J. (1986) Proc. Natl. Acad. Sci. USA 83, 3791–3795.
[29] Worcester, D.L., Michalski, T.J., Tyson, R.L., Bowman, M.K. and Katz, J.J. (1989) Physica B 157, 502–504.
[30] Yoshizawa, H. and Imai, M. (Eds.) (1995) Activity Report on Neutron Scattering Research, Institute for Solid State Physics, University of Tokyo, Vol. 2, 36–38.
[31] Pilz, I. (1969) J. Coll. Interface Sci. 30, 140–144.
[32] Guinier, A. and Fournet, G. (1955) Small Angle Scattering of X-Rays, John Wiley, New York.
[33] Maconnachie, A. and Richards, R.W. (1978) Polymer 19, 739–762.
[34] Donnay, G. (1959) Arch. Biochem. Biophys. 80, 80–85.
[35] Chow, H.-C., Serlin, R. and Strouse, C.E. (1975) J. Am. Chem. Soc. 97, 7230–7242.
[36] Wang, Z.-Y., Marx, G., Umetsu, M., Kobayashi, M., Mimuro, M. and Nozawa, T. (1995) Biochim. Biophys. Acta 1232, 187–196.
[37] Kobayashi, M., Wang, Z.-Y., Yoza, K., Umetsu, Konami, H., Mimuro, M. and Nozawa, T. (1996) Spectrochim. Acta A51, 585–598.
[38] Kratky, C. and Dunitz, J.D. (1977) J. Mol. Biol. 113, 431–442.
[39] Houssier, C. and Sauer, K. (1970) J. Am. Chem. Soc. 92, 779–791.
[40] Katz, J.J., Closs, G.L., Pennington, F.C., Thomas, M.R. and Strain, H.H. (1963) J. Am. Chem. Soc. 85, 3801–3809.
[41] Closs, G.L., Katz, J.J., Pennington, F.C., Thomas, M.R. and Strain, H.H. (1963) J. Am. Chem. Soc. 85, 3809–3821.